Journal of Engineering Physics and Thermophysics, Vol. 82, No. 5, 2009

NUMERICAL ANALYSIS OF THE INFLUENCE OF THE PHYSICAL VISCOSITY ON THE VORTEX HEAT TRANSFER IN LAMINAR AND TURBULENT FLOWS AROUND A HEATED PLATE WITH A SHALLOW SPHERICAL HOLE

S. A. Isaev,[a] S. Z. Sapozhnikov,[b] V. Yu. Mityakov,[b] A. V. Mityakov,[b] S. A. Mozhaiskii,[b] and A. E. Usachov[c]

UDC 532.517.2:4:536.24

The influence of the Reynolds number on the patterns of separation laminar and turbulent flows around a plane plate with a shallow hole as well as on the thermal-hydraulic characteristics of this plate was analyzed on the basis of the solution of the differential mass- and energy-conservation equations, the Navier–Stokes equations, and the Reynolds equations closed with the use of the shear-stress transfer model by the factorized finite-volume method.

Keywords: *vortex heat transfer, numerical simulation, spherical hole, plane plate, RANS, MSST, multiblock computational technologies, VP2/3 package.*

Introduction. Methodical interest in the numerical analysis of the convective heat transfer in a flow around an isolated spherical hole on a plate has increased in the past few years in many respects because of the renewal of systematic physical experiments on new stands (Germany, Australia, Ukraine, and Russia) with the use of modern (PIV) means for diagnostics of vortex flows, gradient transducers of heat flows, and heat-resistant coatings (see, e.g., [1]).

The identification of jet-vortex structures formed in a separation laminar flow of an incompressible viscous fluid around a spherical hole, made in [2–5], lends support to the pattern of this flow obtained earlier as a result of its experimental visualization [6]. It has been shown that, in the case of such a flow around an isolated hole with rounded edges, two symmetric vortex cell are formed on the side surface of the hole and in them there arise self-organizing swirling tornado-like jets interacting in the symmetry plane. From the map of flow regimes obtained in [5] it follows that, as the Reynolds number Re increases from 100 to 2500, a laminar flow without separation around a plane wall with a deep hole (0.2 in fractions of the hole-spot diameter) is changed for the separation one. In this case, a characteristic of the regime of flow without separation is the fluid spreading on the curvilinear wall in the form of smooth continuous tracks of fluid particles deviating into the concavity due to the effect of drawing of fluid into the decreased-pressure zone. The separation of the flow from the rounded edge at Re of the order of 200–300 leads to the formation of local thin bubbles at the lee side of the hole; these bubbles are filled with a practically retarded fluid and initially occupy a very small part of the hole. In the bubbles there arises a weak reverse flow with tracks of particles moving to meet the incident flow. The external flow perceives the bubbles as barriers and bends around them smoothly.

As Re increases to ~700, the motion of the fluid in the separation zone intensifies, and this zone itself becomes thicker and occupies an ever-growing part of the hole. In this case, the reverse flow in the central region of the hole is almost two-dimensional in character, i.e., the streamlines in the neighborhood of the symmetry plane are practically parallel. A Π-shaped vortex is formed in the spherical hole, and in it there arises a mass transfer from the separation zone of the hole through its side windows between the separation line and the line of reattachment of the flow at the windward side of the hole.

Three-dimensional effects arise in the flow at Re of the order of 10^3 when focus-like singular points appear in the pattern of the fluid spreading on the side surface of the hole. At these points there arise spouts in the form of tornado-like swirling jets that initially build into the Π-shaped vortex and then, because of the unwinding of the flow

[a]St. Petersburg State University of Civil Aviation, 38 Pilotov Str., St. Petersburg, 196210, Russia; email: isaev3612@yandex.ru; [b]St. Petersburg State Polytechnical University, 29 Politekhnicheskaya Str., St. Petersburg, 195251, Russia; [c]Moscow Complex TsAGI, 5 Radio Str., Moscow, 107005, Russia. Translated from Inzhenerno-Fizicheskii Zhurnal, Vol. 82, No. 5, pp. 847–857, September–October, 2009. Original article submitted July 28, 2008.

and the decrease in the pressure at the center of the hole, begin to thread the space inside the hole and interact in the symmetry plane. At a later time the separation zone and the windows close (at Re of the order of 1500) and the Π-shaped vortex is transformed into a system of two symmetric vortex cells. At Re = 2500 [3], in a deep spherical hole there arises an intense separation three-dimensional flow with characteristic flow-forming elements: interacting swirling jets passing through the flattened toroidal vortex rings. The paths of fluid particles in the rings represent closed spirals beginning at the center of the hole and running to its periphery along the outer radius and in the reverse direction along the inner radius. It should be noted that, in the above-described numerical investigations of a laminar flow around a spherical hole on a plane, attention was centered on the analysis of the vortex structure formed in a deep ($\Delta = 0.2$) hole with a rounded edge (of the order of 0.1) and problems on the intensification of heat transfer in this flow were practically not considered. Moreover, these investigations were limited by the range of Re numbers (not larger than 2.500) and were carried out on the assumption that the thickness of the boundary layer remains unchanged throughout the depth of the hole.

In [7–20], methodical numerical investigations of a turbulent flow of an incompressible viscous fluid around a spherical hole were carried out for hole depths and Reynolds numbers varying in wide ranges with primary consideration for the intensification of convective heat transfer in the hole. In these investigations prominence was given to the improvement of the computational procedure based on the factorized finite-volume algorithm of solving the Navier–Stokes equations averaged by Reynolds and the substantiation of the choice of the semiempirical model of turbulence. In one of the first works [7] carried out by us jointly with experimenters from the N. E. Bauman Moscow State Technical University, turbulent flow around a shallow spherical hole on a plane plate was calculated with the use of a fairly coarse multiblock grid and a two-parameter dissipative model; it should be noted that the predicted values of the extremum pressure were in fairly satisfactory agreement with the corresponding measurement data. It has been established that even a small concavity on a wall influences substantially the pressure field and gives rise to the formation of a large low-pressure zone into which the fluid from the area surrounding the hole flows.

A further substantial increase in the quality of the numerical simulation of flows was attained due to the development of original multiblock computational technologies realized with the use of the specialized VP2/3 package (velocity–pressure) in the two-dimensional and three-dimensional versions and the model of shear-stress transfer proposed by Menter [21, 22]. The use of intersecting multiblock grids of simple topology made it possible to determine and correctly represent different-scale structural elements of a vortex flow and the temperature field in it. A significant result of the numerical investigations carried out in [9, 10, 18] is establishment of the fact that the vortex structure of a turbulent flow in a deep ($\Delta = 0.22$) hole can experience bifurcation in the case where, depending on the prehistory of the flow, in the hole there arise two symmetric vortex cells similar to the cells formed in the above-considered laminar flow around a spherical hole or an asymmetric single-tornado structure with a transverse flow of fluid from one half of the hole to the other. The bifurcation of a separation flow around a spherical hole is in essence evidence that this flow has a hysteresis nature. The change of a symmetric flow around a spherical hole for the asymmetric one leads to an intensification of the secondary vortex-jet flow and, as a consequence, to a jump-like increase in the heat transfer in the hole and in its neighborhood [13–15]. The disclosure of this effect stimulated the development of asymmetric oval holes inclined at an angle to the incident flow and possessing a higher heat transfer and a better thermal-hydraulic efficiency as compared to the spherical analogs [1, 16, 20, 21].

In a number of works [1, 6, 12, 17, 19], the VP2/3 package and multiblock computational technologies were verified and the choice of the Menter's model of shear-stress transfer modified with account for the curvature of the flow lines within the framework of the Rodi–Leschziner approach with introduction of an additional constant to the function correcting the vortex viscosity [22] was substantiated.

The map of regimes of turbulent flow around a spherical hole [14] illustrating the influence of the depth of the hole on the fluid spreading is by and large analogous to the map of laminar-flow regimes realized at increasing values of Re. However, a significant feature of the turbulent regime of flow is that between the separation and attachment flow lines there arises a window through which fluid flows to the separation zone, i.e., the hole entraps a fluid mass from the incident flow and transfers it through the internal jet flows.

In the present methodical investigation, a uniform flow around a plate heated to 100°C with a spherical shallow hole having a sharp edge ($\Delta = 0.13$) is considered. Unlike the earlier works, prominence is given to the analysis of laminar separation flows with Re > 2500, the comparison of laminar and turbulent flows around the indicated plate

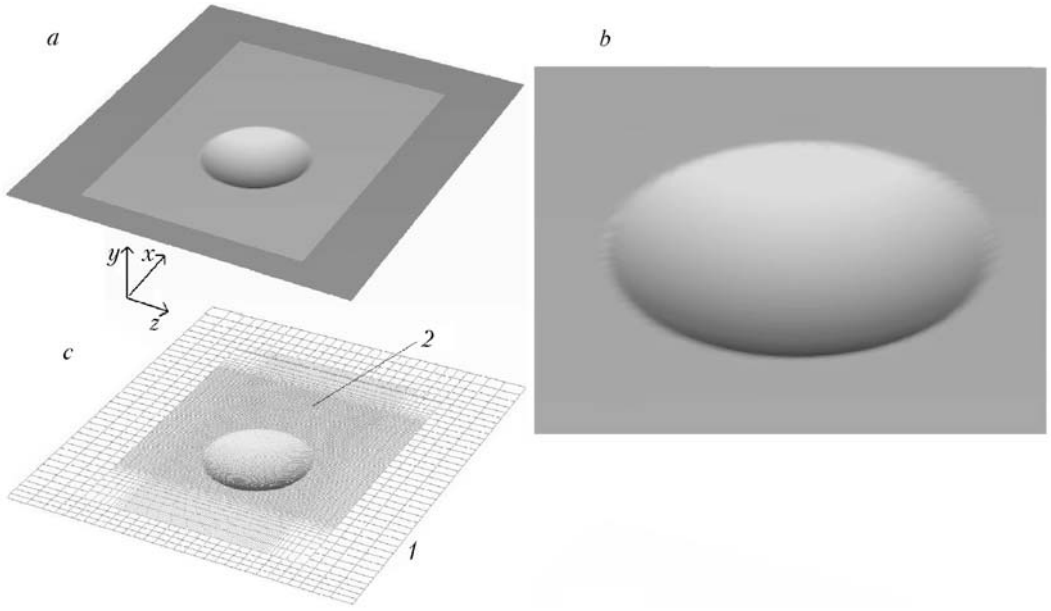

Fig. 1. Plate with a shallow spherical hole with separation zones (a), hole without separation of edges (b), and multiblock grids (c): 1) rectangular grid in the computational region on the plate; 2) oblique grid in the areal of the spherical hole.

for the purpose of determining the role of the hole as a vortex generator, and the estimation of the thermal-hydraulic characteristics of the plate.

Formulation of the Problem and Method of Its Solution. Unlike [12], where a boundless plate with a spherical hole of depth 0.13 was considered and the thickness of the boundary layer at the input of the computational region was prescribed, in the present work, to avoid the difficulties associated with determination of the input boundary conditions, especially in the laminar regime of flow, the conditions corresponding to a uniform air flow with $u = 1$ and $v = w = 0$ are set at the right boundary of the computational region. In this case, the characteristics of turbulence are formulated, as in [12], so that they correspond to the conditions of an aerodynamic experiment: Tu = 1% and the scale of turbulence is of the order of the characteristic size — the diameter of the hole spot d. The Reynolds number selected in accordance with the parameters of the incident flow and the characteristic size varies from $3 \cdot 10^3$ to $2 \cdot 10^4$.

A hole is positioned on a plate of size 3.77×3.4 symmetrically relative to its sides, and the center of the hole is at a distance of 1.53 from the leading edge of the plate (Fig. 1a). The origin of the Cartesian coordinate system x, y, z coincides with the projection of the center of the hole on the plane, and the coordinates of the hole center are 0, −0.13, 0.

The computational region has a height equal to 5. The symmetry conditions are set at the side and upper boundaries of the computational region, and the soft boundary conditions (the conditions of continuation of solution) are set at its output boundary [21]. The adhesion conditions are set at the wall around which the fluid flows.

As in [12], the lower wall is held at a constant temperature $T = 1.273$, and, as the characteristic temperature, a temperature of incident flow equal to 293 K is selected.

The laminar air flow around the plate with a hole and the convective heat transfer in it are calculated at Re numbers changing within the range $3 \cdot 10^3$–$9 \cdot 10^3$ on the basis of solution of the steady-state Navier–Stokes equations for an incompressible viscous fluid and the energy equation by the finite-volume method. For comparison, the turbulent heat transfer near the plate with a hole is calculated at $\mathrm{Re} = 2 \cdot 10^4$. In this case, the steady-state Navier–Stokes equations averaged by Reynolds and the energy equation are solved. The formulation of the problem is described in detail in [21].

TABLE 1. Influence of the Reynolds Number on the Extremum Characteristics of the Flow

Characteristics	Re			
	3000	5000	9000	20 000
u_{min}	–0.163	–0.178	–0.196	–0.220
u_{max}	1.09	1.076	1.07	1.061
w_{min}	–0.089	–0.144	–0.103	–0.143
w_{max}	0.089	0.144	0.209	0.143
v_{min}	–0.04	–0.043	–0.079	–0.060
v_{max}	0.117	0.123	0.179	0.262

The conception of splitting by physical processes forms the basis for the SIMPLEC computational procedure of pressure correction developed for solving the problems on convective heat transfer with the use of partially superimposed multiblock grids.

For decreasing the numerical-diffusion effects, caused by the errors in the approximation of the convective terms of the momentum equation, Leonard's scheme with an upwind quadratic interpolation is used.

The original multiblock computational technologies are realized with the use of the specialized VP2/3 package [21, 22].

The problem is solved with the use of a multiblock computational grid containing cells of the order of 500 thousand. The grid is composed of two different-scale fragments: 1) a rectangular grid with a bunching of nodes to a wall for representation of the flow near the wall; 2) a curvilinear grid adjacent to the wall with a spherical hole, coordinated with the surface of the hole and bunching to the wall (a scalene grid with vertical lines perpendicular to the upper boundary of the computational region). By analogy with [17, 21], the edges of the spherical hole are not separated and a fairly fine grid is constructed in the neighborhood of the hole. This approach seems to be well suited for solving the problem being considered, even though the passage from the spherical surface to the plane wall is not smooth (Fig. 1b).

The subregion in which the grid surrounding the spherical hole is constructed has a length of 3.35 (the center of the hole is at a distance of 1.49 from its input boundary), a width of 2.56, and a height of 0.4. Grids 1 and 2 differ by the spacings between the grid lines, which is determined by the resolution of the structural elements of the flow and the temperature field. The minimum pitches in the longitudinal and transverse directions are taken to be equal to 0.1 for grid 1 and 0.02 for grid 2. The near-wall pitch is equal to 10^{-4}.

The multiblock grid consists of an outer grid containing $39 \times 56 \times 31$ cells, into which a scalene grid with $117 \times 42 \times 91$ cells surrounding the hole is built (Fig. 1c).

Analysis of Results. Some of the results obtained are presented in Figs. 2–6 and in Tables 1 and 2, where data on the local and integral characteristics of the convective heat transfer, including the velocity components, the temperature, the drag C_x, and the heat transfer Nu_m averaged over the area of a separated region of the wall, are collected. The distributions of the relative values of the heat transfer along the longitudinal and transverse coordinates $\overline{Nu}/\overline{Nu}_{pl}$ averaged over the transverse and longitudinal strips of the separated region with a spherical hole are compared. The distributions of the relative values of the local heat transfer Nu/Nu_{pl} over x and z are also compared.

Of particular interest is the evolution of vortex structures in a shallow hole and their correspondence to the physical analogs. As in [6, 9, 10, 16, 21], computer visualization of elements of the vortex-jet structures is performed with the use of the TECPLOT package on the basis of the representation of the spatial trajectories of marked fluid particles passing through definite points of the space.

Before the visualization of the spatial structures of a flow, we constructed the lines of fluid spreading on the surface by analogy with application of a soot-oil coating on the wall around which the fluid flows.

The patterns of fluid spreading in the neighborhood of the shallow hole, shown in Fig. 2, supplement the map of flow regimes presented in [5]. Of course, in this case, a correction for the influence of the depth of the hole (Δ = 0.22 in [5]) should be made; however, in the present work the range of change in Re is much wider.

As was noted above, in the patterns of fluid spreading on the side surface of a spherical hole there arise focus-like singular points, and at $Re = 3 \cdot 10^3$ these points are inside the zone bounded by the line of flow (Fig. 2a). At Re numbers smaller than $5 \cdot 10^3$ (Fig. 2b) the separation laminar flow in the shallow hole is symmetric in character,

TABLE 2. Influence of the Reynolds Number on the Integral Thermal-Hydraulic Characteristics of the Separated Regions

Re	Nu_m	C_x	$Nu_m/Nu_{m.pl}$	C_x/C_{xpl}	HHE
1.5 × 1.5 (region in the wake of the hole)					
3000	10.61 / 11.42	0.0092 / 0.0095	1 / 1.076	1 / 1.032	1 / 1.043
5000	13.54 / 14.7	0.0068 / 0.0071	1 / 1.086	1 / 1.044	1 / 1.040
9000	18.00 / 19.7	0.0049 / 0.0049	1 / 1.094	1 / 1	1 / 1.094
20,000	48.69 / 57.19	0.0060 / 0.0062	1 / 1.175	1 / 1.033	1 / 1.138
1.5 × 1.5 (region surrounding the hole)					
3000	14.26 / 10.52	0.0123 / 0.0105	1 / 0.738	1 / 0.854	1 / 0.864
5000	18.2 / 13.1	0.0092 / 0.0082	1 / 0.720	1 / 0.891	1 / 0.808
9000	24.2 / 17.5	0.0066 / 0.006	1 / 0.723	1 / 0.909	1 / 0.795
20,000	47.86 / 58.6	0.0058 / 0.0148	1 / 1.223	1 / 2.55	1 / 0.480

Note. The values in the numerator were determined at $\Delta = 0$, and the values in the denominator — at $\Delta = 0.13$.

while at $Re = 9 \cdot 10^3$ (Fig. 2c) the symmetric flow in the hole changes to an asymmetric one similar to the turbulent flow in the deep ($\Delta = 0.22$) hole [13–15]. It should be noted that in the experiments carried out at the indicated Reynolds number ($Re = 9 \cdot 10^3$) in a hydraulic channel [23] an analogous regime of laminar flow around a sharp-edge hole with a close depth $\Delta = 0.1$ was detected. A characteristic of a turbulent motion of an incompressible fluid along a wall with a shallow hole, as was shown in [11, 12], is the fluid spreading with the formation of two symmetric vortex cells (Fig. 2d).

It is interesting to analyze how the sizes and the characteristic boundaries of the separation zone change with increase in the Reynolds number. The separation lines on the lee side of the hole are practically coincident with its edges shown by the dashed lines in Fig. 2a–f throughout the range of change in Re. As Re increases from $3 \cdot 10^3$ to $5 \cdot 10^3$, the line of flow attachment at the windward side approaches the trailing edge of the hole, i.e., the sizes of the separation zone increase. Note that at large Reynolds numbers the attachment line has a spiral end.

From Fig. 2g, where the profiles of the longitudinal-velocity components at the center of the hole are compared, it follows that the reverse flow in the hole intensifies, the $u(y)$ profile becomes more filled, and the maximum velocity of the separation flow increases by more than 10% (Table 1) with increase in Re. It is significant that the pattern of fluid spreading on the side surfaces of the hole changes cardinally in this case (Fig. 2e and f). As was earlier noted, windows are formed between the separation and attachment lines. At $Re \le 3 \cdot 10^3$ the windows are opened downwind and fluid is carried out through them from the separation zone (Fig. 2e). The focus-like singular points are inside the zone bounded by the attachment line. At $Re = 5 \cdot 10^3$, on the contrary, the windows are opened to meet the

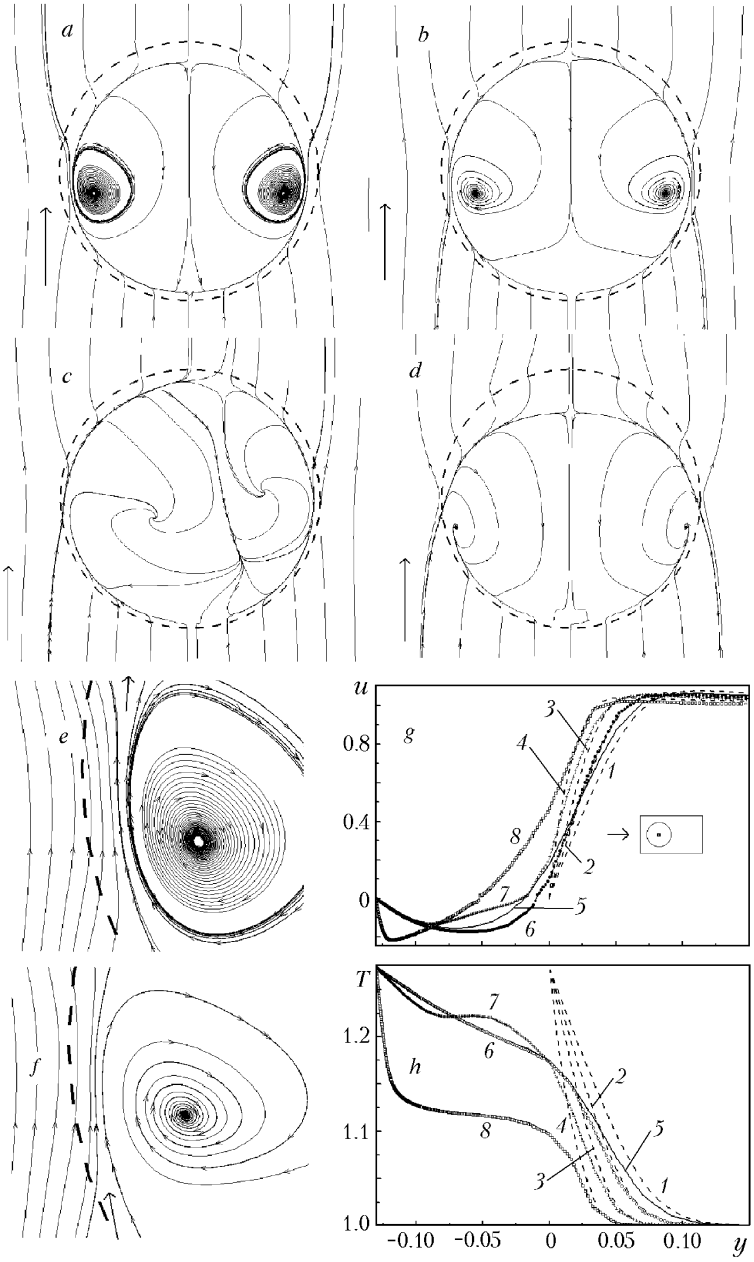

Fig. 2. Patterns of fluid spreading (with separation of edges of the hole) and profiles $u(y)$ (g) and $T(u)$ (h) at the central point of the hole at Re = 3000 (a, e; curves 1, 5 — g, h), 5000 (b, f; 2, 6 — g, h) 9000 (c; 3, 7 — g, h), and $2 \cdot 10^4$ (d; 4, 8 — g, h). The dashed lines 1–4 in Fig. 2g and h correspond to the plane plate.

incident flow; fluid flows through them into the hole and, in doing so, intensifies the circulation flow (Fig. 2f). In this case too, the singular points represent the ends of the separation line.

As Re increases, the sizes of the input windows increase, though, in the asymmetric-fluid-spreading pattern ($\mathrm{Re} = 9 \cdot 10^3$), one window is closed (Fig. 2c) and fluid flows into the hole predominantly from the opened window (positioned on the left side in Fig. 2c). In this case, in the spherical hole there occurs an intensive transverse fluid flow, and a part of the fluid flowing into the hole is drawn in the neighborhood of the singular point found on the right side surface of the hole. By and large the flow in one of the vortex cells becomes more intense than the flows in the other cells, and the sizes of this cell increase significantly.

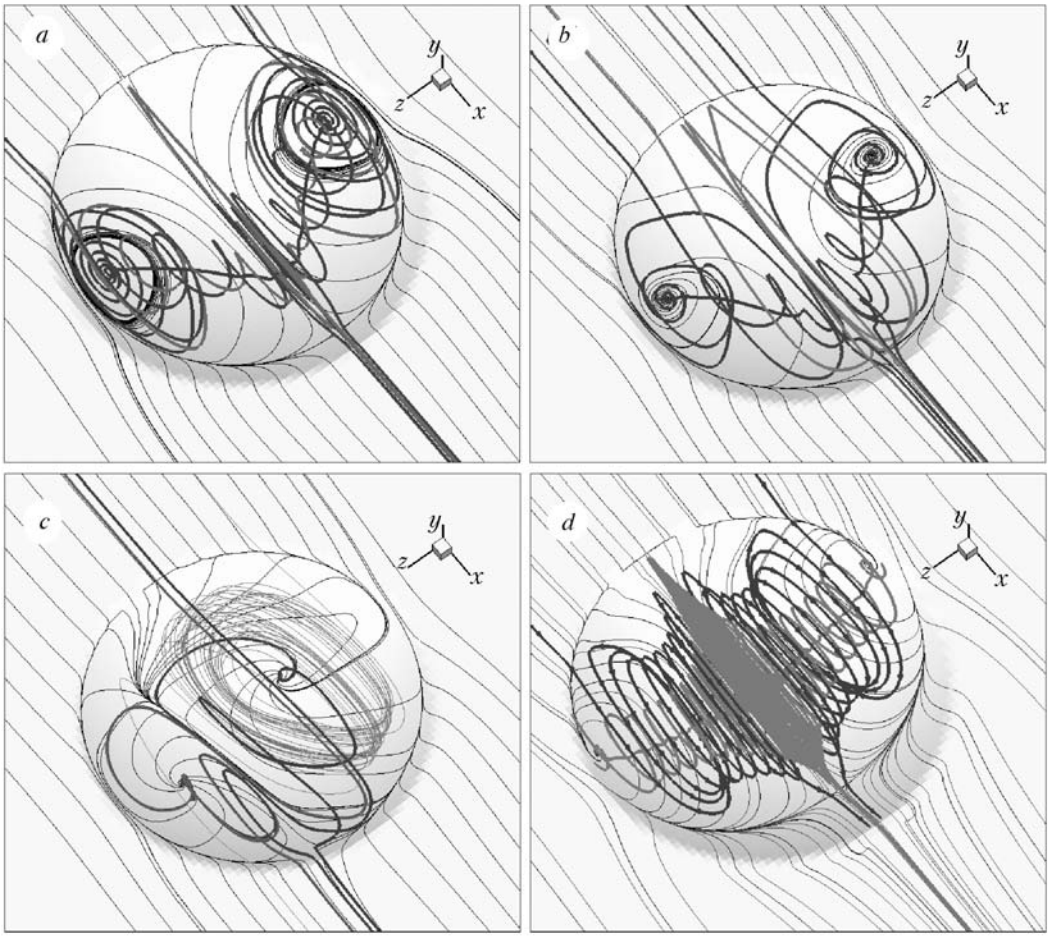

Fig. 3. Influence of Re on the evolution of the vortex-jet structure in the shallow spherical hole: Re = $3\cdot10^3$ (a), $5\cdot10^3$ (b), $9\cdot10^3$ (c), and $2\cdot10^4$ (d).

In the case of a turbulent flow around a shallow hole (Re = $2\cdot10^4$), as in the case of laminar flow at Reynolds numbers smaller than $5\cdot10^3$, the fluid spreading is symmetric (Fig. 2d) with a substantially smaller separation-flow zone. The height and length of this zone is smaller than that for laminar flow (Fig. 2g). At the same time, the input windows on the incident-flow side are much wider and the focus-like singular points are positioned on the lee side of the hole near its edge (Fig. 2d).

The tendency for intensification of a circulation laminar flow in a hole with increase in the Re number, revealed in [5], is retained at $\mathrm{Re} \geq 3\cdot10^3$ (Table 1). Of special note is the increase in the intensity of the secondary flow in the hole ($w_{\max}$ changes from 0.14 to 0.21 with increase in Re from $5\cdot10^3$ to $9\cdot10^3$, and $w_{\max}$ in absolute value is two times larger than $w_{\min}$ and is equal to the maximum, in magnitude, velocity of the reverse flow $u_{\min}$). Not only the transverse-flow velocity, but also the velocities of the downflow and the rising flow, increase in this case. Noteworthy is the fact that, when Re increases, the profile of the velocity of the incident flow changes (Fig. 2g), with the result that the thickness of the boundary layer on the plate decreases markedly, which also influences the intensification of the reverse flow.

As was shown in [21], the asymmetric laminar flow around a spherical hole is much more intense than the symmetric one. At the same time, even though the intensity of the secondary flows decreases (Table 1), the maximum velocity of the reverse turbulent flow in the hole is somewhat higher than that of the laminar flow. Undoubtedly the field of the variable vortex viscosity has a predominant influence on the transfer processes and intensifies them. It was noted in [21] that the hole operating in the turbulent regime plays the role of a turbulence generator influencing, first of all, the heat-transfer processes. As follows from the temperature distributions in the hole, shown in Fig. 2h, turbulization of the flow around the hole cardinally changes the temperature field, with the result that the whole inner re-

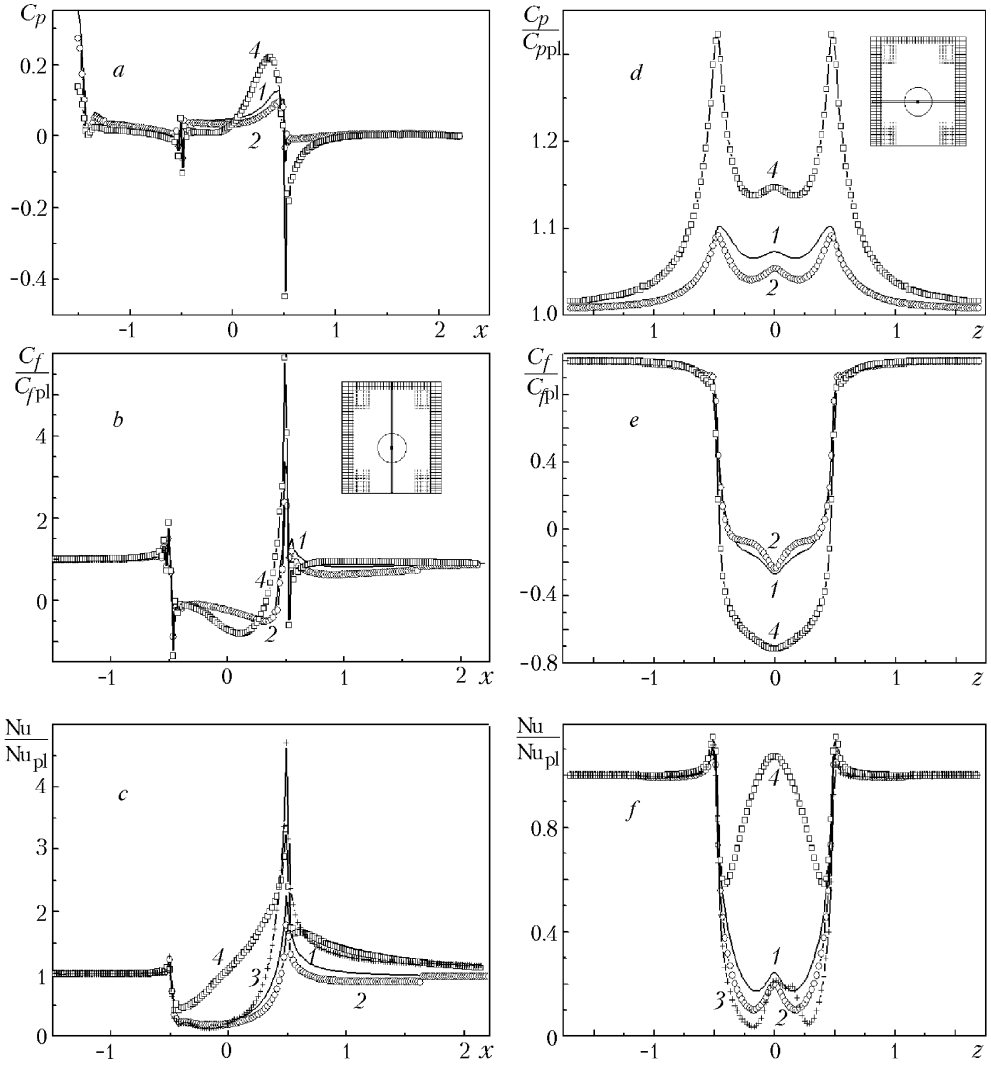

Fig. 4. Influence of the Reynolds number on the distribution of the local characteristics at the longitudinal and transverse middle sections of the plate: $C_p(x)$ (a), $C_f/C_{fpl}(x)$ (b), $Nu/Nu_{pl}(x)$ (c), $C_p/C_{ppl}(z)$ (d), $C_f/C_{fpl}(z)$ (e), $Nu/Nu_{pl}(z)$ (f); $Re = 3\cdot10^3$ (1), $5\cdot10^3$ (2), $9\cdot10^3$ (3), and $2\cdot10^4$ (4).

gion of the hole (and not only the separation zone) is rapidly heated and the heat flows are significantly increased. In this case, the temperature gradient inside the hole is comparable to the temperature gradient at the corresponding point on the plane wall, while this gradient is much smaller for the laminar regime.

As follows from the patterns shown in Fig. 2, the fluid spreading on the side surface of the spherical hole includes singular points. The fluid concentrated at these points flows out from them in the form of swirling jets. Therefore, it is desirable that the given points of the visualization trajectories of marked particles are in the neighborhood of the singular points positioned above the wall. For the patterns shown in Fig. 3 these points have the following coordinates: (–0.062; –0.068; ±0.346), (0.062; –0.03; ±0.346), and (–0.45; –0.03; 0) at $Re = 3\cdot10^3$, (–0.084; –0.058; ±0.36), (–0.084; –0.03; ±0.36), and (–0.45; –0.03; ±0.002) at $Re = 5\cdot10^3$, (–0.074; –0.118; 0.138), (0.029; –0.09; 0.281), (0.029; –0.03; 0.281), and (–0.55; 0.002; –0.3) at $Re = 9\cdot10^3$, (–0.11; –0.022; ±0.44) and (–0.11; –0.022; ±0.22) at $Re = 2\cdot10^4$.

In Fig. 3, on the axonometric projections of the patterns of fluid spreading on the surface of a shallow hole, considered earlier, the spatial tracks of marked particles visualizing the vortex-jet structures of the three-dimensional separation flow around this hole are imposed. In the computer visualization of flows, prominence is given to the for-

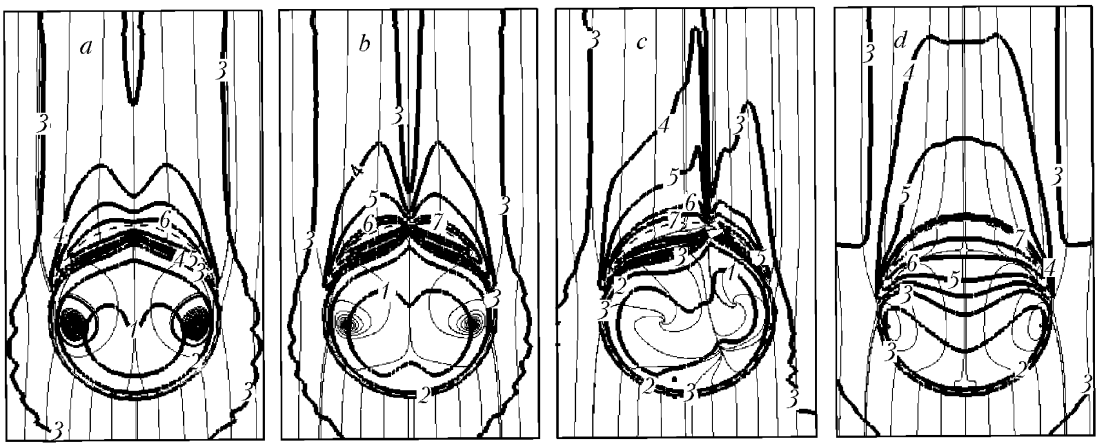

Fig. 5. Influence of Re on the patterns of relative-heat-transfer isolines including fluid-spreading lines: Re = $3\cdot10^3$ (a), $5\cdot10^3$ (b), $9\cdot10^3$ (c), and $2\cdot10^4$ (d). The lines to which numerical values are assigned correspond to Nu/Nu_{pl} = 0.2 (1), 0.6 (2), 1 (3), 1.2 (4), 1.4 (5), 1.8 (6), and 2.2 (7).

mation of tornado-like structures, the centers of which are focus-like singular points in the fluid-spreading patterns. In the case of a symmetric flow in the hole, the jets interact in the symmetry plane and, in doing so, generate a fan jet in its neighborhood. The flow patterns change substantially with increase in Re. As Re increases from $3\cdot10^3$ to $5\cdot10^3$, the axes of the swirling jets in the hole incline at an increasing angle to the incident flow (Fig. 3a and b), and at Re = $5\cdot10^3$ the axis of the jet flowing from a singular point is practically beyond the symmetry plane. It is interesting that marked particles from different regions of the incident flow enter a swirling jet and visualize it. For example, at large Re of the order of $(5–9)\cdot10^3$, particles from the near-wall region of the hole, into which they arrive from the shear layer, enter the swirling jet. The space trajectories of particles in the near-wall layer follow the fluid-spreading lines on the curvilinear wall (Fig. 3c). In the case of an asymmetric flow, the marked particles are carried with a shift from the middle plane of the hole, and in the highly intensive fluid motion in the hole there arises a vortex ring observed earlier in the deep holes at smaller Reynolds numbers [3, 4].

The pattern of a three-dimensional turbulent flow in the hole at Re = $2\cdot10^4$ is similar to the pattern of a laminar flow at a moderate Re number of the order of 10^3. In any event the axes of the interacting jets are inclined at a small angle to the incident flow. The motion of particles in the turbulent flow, unlike that in the laminar flow at Re = $9\cdot10^3$, is ordered in character, i.e., the curvilinear surfaces formed by the paths of the rotating particles are enclosed into each other. It should be noted that a three-dimensional vortex flow of fairly complex topology is realized in the very narrow layer near the wall of the hole, which predetermines the difficulties of its experimental analysis.

The distributions of the local characteristics of a flow and the heat transfer in the longitudinal and transverse cross sections of the shallow hole on the heated plate are presented in Fig. 4. In the case of uniform laminar or turbulent flow at the input of the plate, in the initial region of this gradient-free near-wall flow there arises a zone with a sharply decreasing pressure (Fig. 4a). The distribution $C_p(x)$ in the region of the hole depends substantially on Re and the character of the flow; however, it has typical features. Upstream and downstream of the hole there are low-pressure zones; the pressure in the separation zone is practically constant, and it increases fairly sharply at the windward side.

The negative-friction zones represent the boundaries of the separation zones (Fig. 4b). In a laminar flow, the boundaries of these zones remain practically unchanged when Re increases within the range being considered. When passing to the turbulent regime, the separation zone decreases substantially and its intensity increases. In the vicinity of the trailing sharp edge, C_f experiences a discontinuity: C_f/C_{fpl} increases sharply to 6 at the windward side of the hole, and a local separation takes place on the plane-wall side. In any regime, the flow upstream of the hole accelerates and the differential pressure increases by 1.5–2 times.

The local relative heat transfer $Nu/Nu_{pl}(x)$ at the middle cross section of the plate with a hole decreases sharply within the hole and increases analogously in the wake of it (Fig. 4c). As Re increases, this quantity initially

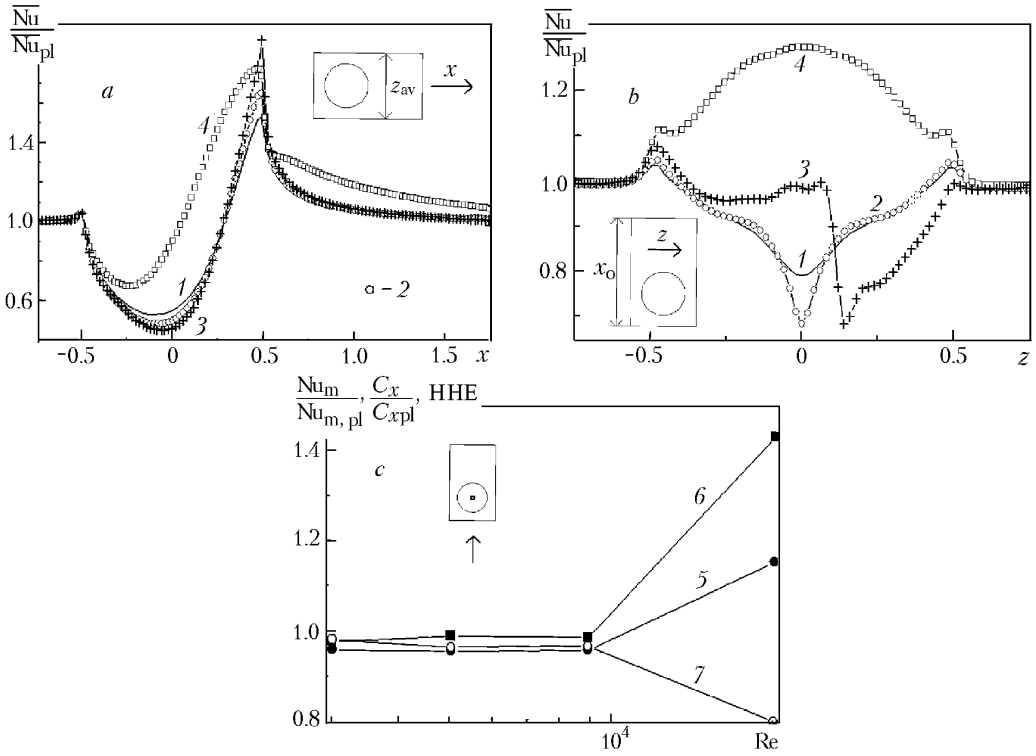

Fig. 6. Influence of Re on the longitudinal (a) and transverse (b) distributions of the $\overline{Nu}/\overline{Nu}_{pl}$ values averaged over the transverse and longitudinal strips of the control region with a hole: Re = $3\cdot10^3$ (1), $5\cdot10^3$ (2), $9\cdot10^3$ (3), and $2\cdot10^4$ (4), and on the integral thermal-hydraulic characteristics of this region (c): 5) $Nu_m/Nu_{m.pl}$; b) C_x/C_{xpl}; 7) heat-hydraulic efficiency (HHE).

decreases in the regime of symmetric laminar flow around the hole and then, in the regime of asymmetric flow, increases sharply. In the case of turbulent flow around the hole, the relative heat transfer at the lee side of the hole is somewhat increased, even though its maximum value in the region of the trailing edge is lower than for the laminar regime at Re = $9\cdot10^3$.

At the transverse middle section of the hole, the differential pressure C_p/C_{ppl} has a local maximum in the region of the side edges (Fig. 4d), the relative friction C_f/C_{fpl} decreases strongly when passing from the laminar regime of flow to the turbulent one (Fig. 4e), and the relative heat transfer $Nu/Nu_{pl}(z)$ increasing by a certain value in the region of the edge (by approximately 8%), in the central region of the hole, and in the laminar regime of flow differs strongly from that in the turbulent regime, even though it retains a local maximum in this region (Fig. 4f). As Re increases, the minimum values of Nu/Nu_{pl} decrease gradually and approach zero, at Re = $9\cdot10^3$ the distribution $Nu/Nu_{pl}(z)$ becomes asymmetric, and in the turbulent regime of flow the maximum value of Nu/Nu_{pl} reaches unity.

As is seen from Fig. 5, in the laminar regime of flow the zone of minimum relative heat transfer in the hole, bounded by curve 1, increases with increase in Re. In the case of turbulent flow around the hole, only in its central region does a fairly narrow region arise with an increased value of Nu/Nu_{pl}. In the other regions the heat transfer exceeds that for the plane wall. In the vicinity of the trailing edge there takes place a peak of Nu/Nu_{pl}, and this peak increases gradually with increase in Re. However, the zone most productive for intensification of heat transfer is in the wake of the hole. When Fig. 5 is analyzed, it is easy to see that, as Re increases, the zone of increased heat loads (e.g., the zone bounded by curve 4 with Nu/Nu_{pl} = 1.2) widens gradually. It is especially large in the turbulent regime of flow (Fig. 5d).

The last-mentioned group of results concerns the integral characteristics of the flow and the heat transfer near the separated region of size 2.5 × 1.5 with a hole (Fig. 6). Analogous results for the region of size 1.5 × 1.5 in the wake of the hole and for the region surrounding the hole (Table 2) were also analyzed.

As in the case of relative local heat transfer in the laminar regime of flow, the value of $\overline{Nu}/\overline{Nu}_{pl}(x)$ averaged over a transverse strip of the region being considered decreases gradually within the hole and, on the contrary, increases in the region of the sharp edge with increase in Re (Fig. 6a). In this case, in the wake of the hole the distributions of $\overline{Nu}/\overline{Nu}_{pl}(x)$ for different values of Re are similar. A turbulization of the flow changes the form of $\overline{Nu}/\overline{Nu}_{pl}(x)$ and leads to a fairly large increase in the total relative heat transfer in the near wake.

Averaging over the longitudinal strips gives a better representation of the intensification of the vortex heat transfer in the region with a hole (Fig. 6b). In the laminar regime of flow the value of $\overline{Nu}/\overline{Nu}_{pl}(z)$ in the vicinity of the middle section of the hole decreases progressively with increase in Re, and this decrease ceases only when an asymmetric flow is realized. However, one can see a region of decreased summarized heat loads on the side of outflow of fluid from the hole (i.e., to the right of the symmetry plane) that cancels, in fact, all the advantages of the heat-transfer intensification in the near wake. The local increase in $\overline{Nu}/\overline{Nu}_{pl}(z)$ in the strip of the hole edges is small (of the order of 10%). In the case of turbulent flow around the hole, the maximum value of $\overline{Nu}/\overline{Nu}_{pl}$ reaches 1.3 at a bell-shaped distribution of the averaged relative heat transfer (Fig. 6b).

Integrating the local force and heat characteristics in the region with a hole, we obtain their average values and determine the heat-hydraulic efficiency of the heat transfer intensification method being considered. As follows from Fig. 6c, these characteristics remain practically unchanged and do not exceed unity in the laminar regime of flow in a wide range of change in Re. In the case of turbulent flow around the hole (at $Re = 2\cdot10^4$), the value of $Nu_m/Nu_{m.pl}$ reaches 1.18, while C_x/C_{xpl} increases to 1.43. Thus, the heat-hydraulic efficiency is smaller than unity and is equal to 0.8.

It is interesting to analyze the reasons for such behavior of the average characteristics with change in Re. For this purpose we will consider the data presented in Table 2. It may be suggested that the separated region of size 1.5 × 1.5 positioned in the wake of the hole and making contact with its edge has a minimum aerodynamic drag. At the same time, as already noted, it is in this region that the zone of increased heat loads is located. As a result, as Re increases in the laminar flow, $Nu_m/Nu_{m.pl}$ increases monotonically from 1.08 to 1.09 and C_x/C_{xpl} does not exceed 1.03–1.04. Thus, a fairly moderate intensification of heat transfer takes place, and the heat transfer increases ahead of the aerodynamic losses. In the spherical hole, on the contrary, $Nu_m/Nu_{m.pl}$ does not exceed 0.72–0.74 and C_x/C_{xpl} changes in the range 0.85–0.91. Thus, the hole gives rise to a significant cooling effect along with a decrease in the aerodynamic losses.

The increase in $Nu_m/Nu_{m.pl}$ in the wake of the hole in the turbulent regime of flow is larger than that in the laminar regime and is equal to 1.18 at a small increase (of 1.03) in the relative aerodynamic load. The increase in $Nu_m/Nu_{m.pl}$ within the hole is larger than that in the zone positioned in the wake and is equal to 1.22, and C_x/C_{xpl} increases by a larger value — by 2.55 times. It is precisely this circumstance that explains the low thermohydraulic characteristics of the region of the plate with a shallow spherical hole.

Conclusions. A comparative numerical analysis of the vortex dynamics and the heat transfer in the uniform laminar and turbulent air flows around a plate heated to 100°C with a shallow spherical hole has been carried out. Prominence was given to large Reynolds numbers changing within the range from $3\cdot10^3$ to $9\cdot10^3$. The map of flow regimes was widened and the vortex-jet structures in the hole were identified. It has been established that the symmetric fluid spreading on the side surface of the hole is transformed when the Re number increases from $3\cdot10^3$ to $5\cdot10^3$: the focus-like singular points that are initially on the line of attachment of the separation flow then become the ends of the separation line. As a result, windows are formed. Through these windows the air from the near-wall layer flows to the hole and, in doing so, intensifies the circulation flow. At $Re = 9\cdot10^3$, the fluid spreading becomes asymmetric, and the intensity of the secondary flows caused by the transverse motion of the medium in the hole increases substantially. In the turbulent regime of flow at $Re = 2\cdot10^4$ the length of the separation-flow zone in the hole decreases substantially and, in it, a symmetric vortex structure is formed once again. Even though the intensity of the circulation flow in the hole increases insignificantly as compared to that in the laminar regime of flow at $Re = 9\cdot10^3$, the zone of increased relative local heat loads inside the hole and in the areal surrounding it increases substantially, which points to the fact that the hole plays an important role as a vortex generator. By and large, in the case of laminar flow around the region with a shallow hole, the heat transfer from this region does not increase and aerodynamic losses do not arise. The relative local heat losses inside the hole are very small (close to zero). In the turbulent regime of flow

around the region with a hole of size 2.5 × 1.5, the relative heat transfer from this region increases moderately (by approximately 18%), with the result that the total drag increases ahead of the losses to 1.43.

This work was carried out with financial support from the Russian Foundation for Basic Research (projects No. 07-08-00635, 08-08-00065, and 08-01-00059) and DFG HA 2226/11-1.

NOTATION

C_f, coefficient of friction; C_p, pressure coefficient; C_x, drag coefficient of the plate region with a hole; d, diameter of the spherical-hole spot, m; Nu, Nusselt number; Re, Reynolds number, Re = $\rho Ud/\mu$; T, temperature in fractions of 293 K; U, velocity of the incident flow, m/sec; u, v, w, longitudinal, vertical, and transverse components, in fractions of U; x, y, z, longitudinal, vertical, and transverse coordinates, in fractions of d; Δ, depth of a spherical hole, in fractions of d; μ, coefficient of dynamic viscosity, kg/(m·sec); ρ, density, kg/m^3; HHE $\approx (\mathrm{Nu_m}/\mathrm{Nu_{m.pl}})/(C_x/C_{x\mathrm{pl}})$. Subscripts: $\bar{}$, quantities averaged over the separated strip; av, separated-strip size over which the averaging is performed; min, max, minimum and maximum quantities; m, parameters averaged over the area of a region; pl, plane wall.

REFERENCES

1. J. Turnow, N. Kornev, S. Isaev, and E. Hassel, Vortex-jet mechanism of heat transfer enhancement in a channel with spherical and oval dimples, *Proc. Int. Conf. on Jets, Wakes and Separated Flows*, Berlin (2008).
2. S. A. Isaev, A. I. Leont'ev, and A. E. Usachov, Numerical study of the eddy mechanism of enhancement of heat and mass transfer near a surface with a cavity, *Inzh.-Fiz. Zh.*, **71**, No. 3, 484–490 (1998).
3. S. A. Isaev, A. I. Leont'ev, D. P. Frolov, and V. B. Kharchenko, Identification of self-organizing vortex structures in numerical modeling of a three-dimensional laminar viscous incompressible fluid flow around a hole on a plane, *Pis'ma Zh. Tekh. Fiz.*, **24**, Issue 6, 6–11 (1998).
4. S. A. Isaev, A. I. Leont'ev, A. E. Usachov, and D. P. Frolov, Identification of self-organizing jet-vortex structures in numerical modeling of a laminar flow and heat transfer in the vicinity of an isolated asymmetric hole, *Izv. Ross. Akad. Nauk, Énergetika*, No. 2, 126–136 (1999).
5. S. A. Isaev, A. I. Leont'ev, P. A. Baranov, Kh. T. Metov, and A. E. Usachov, Numerical analysis of the effect of viscosity on the vortex dynamics in laminar separated flow past a dimple on a plane with allowance for its asymmetry, *Inzh.-Fiz. Zh.*, **74**, No. 2, 62–67 (2001).
6. S. A. Isaev, I. A. Pyshnyi, A. E. Usachov, and V. B. Kharchenko, Verification of the multiblock computational technology in calculating laminar and turbulent flow around a spherical hole on a channel wall, *Inzh.-Fiz. Zh.*, **75**, No. 5, 122–124 (2002).
7. S. A. Isaev, V. B. Kharchenko, and Ya. P. Chudnovskii, Calculation of a three-dimensional flow of a viscous incompressible liquid in the neighborhood of a shallow well, *Inzh.-Fiz. Zh.*, **67**, Nos. 5–6, 373–378 (1994).
8. S. A. Isaev, A. I. Leont'ev, and A. E. Usachov, Methodological aspects of numerical simulation of the dynamics of the vortex structures and heat transfer in viscous turbulent flows, *Izv. Ross. Akad. Nauk, Énergetika*, No. 4, 140–148 (1996).
9. S. A. Isaev, A. I. Leont'ev, and P. A. Baranov, Identification of self-organizing tornado-like structures in numerical simulation of a turbulent viscous incompressible fluid flow around a hole on a plane, *Pis'ma Zh. Tekh. Fiz.*, **26**, Issue 1, 30–36 (2000).
10. S. A. Isaev, A. I. Leont'ev, P. A. Baranov, and A. E. Usachov, Bifurcation of a vortex turbulent flow and intensification of heat transfer in a hole, *Dokl. Ross. Akad. Nauk*, **373**, No. 5, 615–617 (2000).
11. S. A. Isaev, A. I. Leont'ev, Kh. T. Metov, and V. B. Kharchenko, Modeling of the influence of viscosity on the tornado heat exchange in turbulent flow around a small hole on the plane, *Inzh.-Fiz. Zh.*, **75**, No. 4, 98–104 (2002).
12. P. A. Baranov, S. A. Isaev, A. I. Leont'ev, A. V. Mityakov, V. Yu. Mityakov, and S. Z. Sapozhnikov, Physical and numerical simulation of the vortex heat transfer in a turbulent flow around a spherical hole on a plane, *Teplofiz. Aéromekh.*, **9**, No. 4, 521–532 (2002).

13. S. A. Isaev, A. I. Leont'ev, N. A. Kudryavtsev, and I. A. Pyshnyi, On the influence of the rearrangement of a vortex structure with increase in the depth of a spherical hole on the wall of a narrow plane-parallel channel on the jumpwise change in the heat transfer, *Izv. Ross. Akad. Nauk*, *Teplofiz. Vys. Temp.*, **41**, No. 2, 268–272 (2003).
14. S. A. Isaev and A. I. Leont'ev, Numerical simulation of the vortex intensification of heat transfer in turbulent flow around a spherical hole on the wall of a narrow channel, *Izv. Ross. Akad. Nauk*, *Teplofiz. Vys. Temp.*, **41**, No. 5, 755–770 (2003).
15. S. A. Isaev, A. I. Leont'ev, P. A. Baranov, and I. A. Pyshnyi, Numerical analysis of the influence of the depth of a spherical hole on a plane wall on the turbulent heat exchange, *Inzh.-Fiz. Zh.*, **76**, No. 1, 52–59 (2003).
16. S. A. Isaev, A. I. Leont'ev, A. V. Mityakov, and I. A. Pyshnyi, Intensification of tornado turbulent heat exchange in axisymmetric holes on a plane wall, *Inzh.-Fiz. Zh.*, **76**, No. 2, 31–34 (2003).
17. S. A. Isaev, A. I. Leont'ev, G. I. Kiknadze, N. A. Kudryavtsev, and I. A. Gachechiladze, Comparative analysis of the vortex heat exchange in turbulent flow around a spherical hole and a two-dimensional trench on a plane wall, *Inzh.-Fiz. Zh.*, **78**, No. 4, 117–128 (2005).
18. N. Kornev, E. Hassel, H. Herwig, S. Isaev, P. Stephan, and V. Zhdanov, Enhancement of heat transfer from dimpled surfaces by the use of vortex induction, *Eng. Res.* (*Forschung im Ingenieurwesen*), **69**, No. 2, 90–100 (2005).
19. S. A. Isaev, A. I. Leont'ev, and P. A. Baranov, Simulation tornado-like enhancement of heat transfer for low-velocity motion of air in a rectangular channel with cavities. Pt. 1: Selection and justification of calculation methods, *Thermal Eng.*, **54**, No. 3, 193–199 (2007).
20. S. A. Isaev, A. I. Leont'ev, and P. A. Baranov, Simulation tornado-like enhancement of heat transfer for low-velocity motion of air in a rectangular channel with cavities. Pt. 2: Results of parametric studies, *Thermal Eng.*, **54**, No. 8, 655–663 (2007).
21. Yu. A. Bystrov, S. A. Isaev, N. A. Kudryavtsev, and A. I. Leont'ev, *Numerical Simulation of the Vortical Intensification of the Heat Transfer in Stacks of Tubes* [in Russian], Sudostroenie, St. Petersburg (2005).
22. V. B. Kharchenko, *Numerical Simulation of Separation Flows with Vortex and Jet Generators on the Basis of Multiblock Computational Technologies* [in Russian], Author's Thesis of Doctoral Dissertation (in Engineering), St. Petersburg (2006).
23. A. A. Khalatov, *Heat Transfer and Hydrodynamics Near Surface Depressions* (*Holes*) [in Russian], ITTF, Kiev (2005).